Population co-exposure to extreme heat and wildfire smoke pollution in California during 2020

ENVIRONMENTAL RESEARCH
CLIMATE

OPEN ACCESS

RECEIVED
21 May 2022

REVISED
20 July 2022

ACCEPTED FOR PUBLICATION
2 August 2022

PUBLISHED
25 August 2022

PAPER

Population co-exposure to extreme heat and wildfire smoke pollution in California during 2020

Noam Rosenthal[1,*], Tarik Benmarhnia[2], Ravan Ahmadov[3], Eric James[3] and Miriam E Marlier[4]

[1] University of California Los Angeles, Institute of the Environment and Sustainability, LaKretz Hall, 619 Charles E Young Dr E, Los Angeles, CA 90095-1772, United States of America
[2] University of California San Diego Scripps Institution of Oceanography, 8622 Kennel Way, La Jolla, CA 92093-5004, United States of America
[3] University of Colorado Boulder, Cooperative Institute for Research in Environmental Sciences, 325 Broadway, Boulder, CO 80309-0401, United States of America
[4] Department of Environmental Health Sciences, University of California Los Angeles Jonathan and Karin Fielding School of Public Health, 650 Charles Young Dr S, Los Angeles, CA 90095-1772, United States of America
* Author to whom any correspondence should be addressed.

E-mail: noamr@g.ucla.edu

Keywords: extreme heat, wildfire smoke, exposure, compounding hazards

Supplementary material for this article is available online

Abstract

Excessive warming from climate change has increased the total wildfire burned area over the past several decades in California. This has increased population exposure to both hazardous concentrations of air pollutants from fires such as fine particulate matter (smoke $PM_{2.5}$) and extreme heat events. Exposure to $PM_{2.5}$ and extreme heat are individually associated with negative health impacts and recent epidemiological evidence points to synergistic effects from concurrent exposures. This study characterizes the frequency and spatial distribution of co-occurring extreme heat and smoke $PM_{2.5}$ events in California during the record-setting wildfire season of 2020. We measure exceedances over extreme thresholds of modeled surface-level smoke $PM_{2.5}$ concentrations and heat index based on observed temperature and humidity. We estimate that, during the studied period, extreme smoke and heat co-occurred at least once within 68% of the state's area (~288 000 km^2) and an average 2.5 times across all affected areas. Additionally, 16.5 million people, mostly in lower population density areas, were impacted at least once in 2020 by such synergistic events. Our findings suggest that public health guidance and adaptation policies should account for co-exposures, not only distinct exposures, when confronting heat and smoke $PM_{2.5}$.

1. Introduction

An increase in the frequency and severity of climate-related hazards has renewed interest in the distribution of multi-hazard events that can produce extraordinary risks (Field *et al* 2012). Hazards may coincide in space and time by random chance, shared meteorological drivers or causal interdependency (Zscheischler *et al* 2020). Examples include a flood after an earthquake; the co-occurrence of extreme wind and flooding during severe storms (Nielsen *et al* 2015); or the increased likelihood of landslides in wildfire-damaged areas, respectively (Mazdiyasni and AghaKouchak 2015, Moftakhari *et al* 2017). Whereas multi-hazard systems have been examined theoretically, empirical characterizations of their dynamics and drivers, not least in the wildfire pollution context, are more limited (Gill and Malamud 2014).

Wildfires contribute to increased trace gas and aerosol concentrations that are harmful to human health. Fine particulate matter contributed by fires ('smoke $PM_{2.5}$'; particles smaller than 2.5 μms in diameter) is particularly dangerous because it directly enters bloodstreams and alveoli, impairing cardiorespiratory functions (Brook *et al* 2010, Guo *et al* 2018) as well as other organs such as the brain (Weuve *et al* 2021). Moreover, in comparison with $PM_{2.5}$ from other sources, researchers have identified distinct mutagenic and

oxidative stresses in humans from smoke $PM_{2.5}$ (Nakayama Wong *et al* 2011, DeFlorio-Barker *et al* 2019, Aguilera *et al* 2021). In the western United States and California, smoke $PM_{2.5}$ was found to increase respiratory hospitalizations by as much as 7% and 3.3%, respectively, over a six-year period (Liu *et al* 2017, Heaney *et al* 2022).

While all-source $PM_{2.5}$ concentrations declined in the Eastern United States from 2006–2016, many areas in the west experienced an increase in $PM_{2.5}$ attributable to summertime wildfires that offset declines in non-fire anthropogenic sources (O'Dell *et al* 2019). Wildfire smoke accounted for as much as half of the overall $PM_{2.5}$ exposure in the western United States in recent years, compared to approximately 20% on average in the mid-2000s (Burke *et al* 2021). Future climate scenarios project that, by 2100, wildfire smoke will account for more than 50% of total $PM_{2.5}$ across the entire continental United States (Ford *et al* 2018).

Extreme heat often precedes fire ignition as high temperatures predispose vegetational fuels to ignite and burn (Goss *et al* 2020). Heat presents a sizable health risk of its own; it elevates heart and respiratory rates as well as blood viscosity and cholesterol, which may aggravate pre-existing conditions (Keatinge *et al* 1986, Davies and Maconochie 2009, Sherbakov *et al* 2018, Cheng *et al* 2019, Ebi *et al* 2021). In California, select heat waves have been estimated to cause as much as a 6% increase in excess deaths (Hoshiko *et al* 2010) and as much as a 39% and 47% increase in the likelihood of hospitalization for dehydration and renal failure, respectively (Schwarz *et al* 2020).

Rising global temperatures and more frequent extreme heat events are expected to increase wildfire size and intensity, signaling a growing public health threat from concurrent heat-smoke exposure (Perkins *et al* 2012, Abatzoglou and Williams 2016, Westerling 2018). However, exposure inventories of heat-smoke co-occurrence (HSC) that include smoke $PM_{2.5}$, which would help elucidate the drivers of hospitalization and death, are comparatively scarce. Austin *et al* (2020) examined exposure to HSC among outdoor agricultural workers at the county level in Washington and found strong spatiotemporal variability in areas exposed to high heat and high levels of $PM_{2.5}$, and that these exposures occured prima during the summer wildfire season (Austin *et al* 2020). More recently, researchers examined the co-occurrence of heat, ozone and $PM_{2.5}$ in the Western United States (Kalashnikov *et al* 2022). These two studies, however, used concentration measurements that include all sources of $PM_{2.5}$ (versus smoke-specific $PM_{2.5}$) and relied on either unevenly distributed air quality stations or a coarse 10 km resolution, respectively. These spatially coarse measures of compound exposure constrain policymaking because they preclude investigation into the sociodemographic correlates of exposure (Schwarz *et al* 2021).

In this study, we investigate the frequency, intensity and duration of individual and combined extreme heat and smoke $PM_{2.5}$ exposures in California from June through November 2020. During this time period wildfires burned over four million acres—the largest burned area in the State's recorded history dating back to 1878—and coincided with the fourth hottest summer since 1895 (CalFire 2020, National Centers for Environmental Information 2020). Our analysis is done at a 3 km spatial resolution and maps single and compound hazard exposures at surface level across different population characteristics, including race, ethnicity, income and health, to identify the communities most exposed to HSC. We contribute to the literature of compound climate exposures in California by: (a) modeling smoke $PM_{2.5}$ rather than total $PM_{2.5}$ to isolate fire contributions, (b) mapping compound exposures at fine spatial scale, and (c) identifying sociodemographic correlates of exposure.

2. Materials and methods

2.1. Smoke $PM_{2.5}$ exposure

We quantify smoke pollution exposure using NOAA's High-Resolution Rapid Refresh coupled with smoke (HRRR-Smoke) atmospheric model. Based on the Weather Research and Forecasting model coupled to Chemistry model, HRRR-Smoke provides surface-level smoke $PM_{2.5}$ estimates across the United States in near real-time. Fire emissions estimates are based on satellite observations of fire radiative power as detected by the Visible Infrared Imaging Radiometer Suite (VIIRS) and Moderate Resolution Imaging Spectroradiometer (MODIS) satellites (Ahmadov *et al* 2017). The model is initialized every 12 h at a 3 km horizontal grid spacing; for this study, we utilize 48 h forecasts initialized at 00 and 12 UTC. HRRR-Smoke $PM_{2.5}$ estimates do not account for non-fire sources of pollution (from traffic, industry, etc) and are therefore specific to fire contributions only. Previous validation of HRRR-Smoke with all-source ground station measurements during the 2018 Camp Fire identified strong spatiotemporal agreement with observed progressions of smoke plume locations and magnitudes (Chow *et al* 2021).

We use the average of 24 individual hourly HRRR-Smoke forecasts to estimate daily smoke $PM_{2.5}$. All hourly concentration forecasts are based on the most recent available 00 or 12 UTC model initialization ($n = 364$) given the increased accuracy of meteorological conditions closer to the forecast. In the event that an initialization is skipped ($n = 57$) predictions from the most proximate initialization timestamp are used

(i.e. the previous day's forecasts). Following this correction there are 3 d, out of 182 total, that are missing data for all initializations. These gaps, resulting from computer outages during the model run, are omitted from our analysis.

In the absence of smoke-specific observed $PM_{2.5}$ mass concentrations, we compare HRRR-Smoke forecasts with a network of 166 ground station all-source $PM_{2.5}$ measurements managed by the EPA's Air Quality System (AQS) (figure S4). This dataset is an imperfect validation dataset since it includes anthropogenic sources of $PM_{2.5}$ in addition to wildfire smoke. However, during extreme smoke events when wildfire contributions dominate, AQS measurements may converge towards HRRR-Smoke estimates. AQS measurements are sourced from national, state and local air stations associated with parameter codes 88 502 and 88 101, providing daily average $PM_{2.5}$ concentrations from all sources (US EPA O 2014). The point geometries of AQS stations are coupled with gridded HRRR-Smoke estimates based on their intersection.

2.2. Temperature exposure

Extreme heat exposures are calculated from the Gridded Surface Meteorological dataset (GRIDMET) that includes daily surface measurements of maximum and minimum temperature, humidity and other meteorological variables across the contiguous United States (Abatzoglou 2013). We resampled the data from its original 4 km resolution to 3 km to align with HRRR-Smoke output. Humidity and temperature are combined to estimate apparent temperature or heat index, a stronger correlate of biological heat stress that is referenced by the federal Occupational Safety and Health Administration in its exposure guidelines (Jacklitsch *et al* 2016). We follow the National Weather Service's Weather Prediction Center's method, which adapts the Rothfusz regression model (equation (1)) to account for more extreme conditions and is reported in Fahrenheit (Rothfusz 1990, National Weather Service 2014):

$$\begin{aligned}\text{Daily Maximum Heat Index} = {} & -42.379 + 2.04901523T + 10.14333127R - 0.22475541TR \\ & - 6.83783 \times 10^{-3}T^2 - 5.481717 \times 10^{-2}R^2 + 1.22874 \times 10^{-3}T^2R \\ & + 8.5282 \times 10^{-4}TR^2 - 1.99 \times 10^{-6}T^2R^2 \end{aligned} \quad (1)$$

where:
T = Daily Maximum Temperature (°F)
R = Daily Minimum Relative Humidity (%).

These heat index measurements are then used to identify 'exceedances' for our population exposure analysis (see section 2.3). Previous validation work found the median correlations between GRIDMET and a national sample of over 1500 remote automated weather stations to be 0.94–0.95 and 0.87–0.90 for maximum and minimum temperature, respectively, with median mean absolute error (MAE) between 1.7 °C and 2.3 °C. Daily maximum and minimum RH featured median correlation values between 0.77 and 0.81 and median MAE between 6% and 12% (Abatzoglou 2013).

2.3. Exceedance thresholds

We define an extreme smoke exposure event as any day with 24 h smoke $PM_{2.5}$ exceeding 20 $\mu g\ m^{-3}$. Our threshold of 20 $\mu g\ m^{-3}$ corresponds to the 98th percentile of smoke $PM_{2.5}$ measured by a global atmospheric chemistry model across the western United States between 2004–2009 (Liu *et al* 2017). Finally, we define a *smoke wave*, designed to be analogous to a heatwave, as two or more consecutive exceedances. This accounts for the potential risks of sporadic, yet persistent, exposure to high concentrations of smoke $PM_{2.5}$ that are common during long-lasting conflagrations (Liu *et al* 2017).

For heat, we define an extreme threshold as the greater of two prespecified intensity values. First, we calculate the 85th percentile historical heat index for the months of July and August, within a grid cell, for 1970–2010 (US EPA O 2021). This location-specific threshold accounts for any local behavioral or physical adaptations to extreme heat. Second, we apply an absolute minimum heat index cutoff of 80 °F for daily maximum temperatures, which corresponds to the National Institute for Occupational Safety and Health's lowest 'caution' heat-index for worker safety (Jacklitsch *et al* 2016). Accordingly, colder areas where the summertime 85th percentile corresponds to a mild temperature will instead be compared to an absolute cutoff. Conversely, to avoid 'false negatives', we also apply an absolute maximum heat index cutoff of 105 °F for areas with extreme summertime 85th percentile historical heat indices; this threshold corresponds to the National Weather Service's excessive heat warning trigger. Finally, in addition to single event exceedances, we adopt a definition of *heat wave* as two or more consecutive exceedances in a given location.

Using Google Earth Engine, a cloud-based geocomputation engine, we intersect both hazard exceedances to identify HSC at a daily interval at a resampled scale of 3 km (Gorelick *et al* 2017). Since there are no standardized definitions for extreme heat or extreme smoke, we further analyze the sensitivity of our results to different definitions: for temperature we increase the threshold to the 95th percentile and for smoke we

test an absolute cutoff of 35 μg m^{-3}, which corresponds to the EPA's 24 h national ambient air quality standard for all source $PM_{2.5}$ (US EPA O 2014). Finally, we test the differences between using daily maximum and minimum heat indices for temperature percentile thresholds as well as the impact of focusing only on persistent exceedances (smoke waves or heat waves). These alterations are informed by evidence of hotter evening temperatures and persistent heat exposure increasing morbidity and mortality (Rey *et al* 2007, Zhang *et al* 2012).

2.4. Population characteristics

To quantify total human exposure and the density of affected areas, population data are taken from Gridded Population of the World Version 4.11, which is an interpolation of decennial census population counts at a 1 km resolution (CIESIN 2018, OEHHA 2021). Additionally, we use California's Office of Environmental Health Hazard Assessment CalEnviroScreen 4.0 and the 2019 5 year American Community Survey to measure existing pollution burdens and socioeconomic characteristics for all census tracts across the State, respectively (U.S. Census Bureau 2019) (figure S5). We resolve spatial mismatch between the 3 km hazard layer and variably sized census tracts by computing the aggregated hazard metrics within a 9 km radius (3×3 pixel window) of each census tract's centroid.

We also measure the correlation between each hazard's magnitude and the prevalence of different sociodemographic variables. Each variable is first ranked and binned into deciles and then the mean magnitude exceedance is computed for each hazard in a given census tract's vicinity for each bin. For analyses related to population exposure (incidence), where we compute the relative ratio between a group's share of the HSC impacted population and their share of the total state population, we sum population counts for each census tract in proportion to the area of the tract affected at least once by HSC.

3. Results

3.1. HRRR-smoke model comparison

In comparison with the EPA's AQS network of ground stations, smoke $PM_{2.5}$ concentrations simulated by the HRRR-Smoke model were typically lower than all-source $PM_{2.5}$ station measurements; the median HRRR-Smoke grid cell estimate corresponding to each site was 0.4 μg m^{-3} versus 10.0 μg m^{-3} for AQS. This difference is expected since AQS accounts for all sources of $PM_{2.5}$ most days do not feature any smoke pollution and a majority of the AQS stations are located in urban areas with heavier anthropogenic contributions. Indeed, biases between AQS and HRRR-Smoke were highest in less populated areas and lowest in urban areas where car exhaust and residential gas appliances, for example, dominate $PM_{2.5}$ emissions (figure S2). The correlation coefficient between both datasets, which was greatest for same day comparisons without lag, equaled 0.62, indicating sufficient temporal coherence. When comparing all AQS measurements with the nearest HRRR-Smoke forecast, the normalized MAE (NMAE) equaled 77%; after filtering for 'extreme' HRRR-Smoke forecasts (>20 μg m^{-3}) NMAE drops to 60%. These statistics match reported metrics for previous comparisons with smoke-enhanced aerosol optical depth measurements during the Williams Flats Fire in 2019 (Ye *et al* 2021).

3.2. Spatiotemporal trends

Both hazards co-occurred at least once across 288 505 km^2 (~68%) of California during the 2020 study period (figure 1). The statewide average of the season's maximum observed exceedance over the baseline thresholds was 3.0 °F for the daily maximum heat index and 51.1 μg m^{-3} for smoke $PM_{2.5}$. The latter is more than twice the smoke event threshold and almost 150% above the EPA 24 h standard of 35 μg m^{-3}. Notably, exceedance magnitudes during compounding events were lower for temperature, averaging 2.6 °F. Smoke exceedances were also lower during HSC events, averaging 40.9 μg m^{-3}.

HSC occurred a maximum of seventeen times across four different grid cells in California's Carmel Valley and for as long as nine consecutive days along the western edge of the Mojave Desert, southeast of Sequoia National Park. The Monterey Bay area was also one of the most frequently affected areas in the state. Most co-occurrences coincided spatiotemporally with season's most severe conflagrations (figure 2) including the August Complex, North Complex and Creek Fires that affected the Northern California coastline, Upper Sierras and Central Valley, respectively.

We also identified trends across the four Level 1 North American ecoregions in California which are: Mediterranean California (Mediterranean), North American Deserts (Desert), Marine West Coast Forests (Marine) and Northwestern Forested Mountains (Forested). These ecoregions delineate distinct ecologies and climates that can affect smoke production and temperature (figure S1) (Omernik 1987). California's Marine and Forested ecoregions were the two most affected by HSC, with nearly equal frequency-weighted impacted areas of 1.2%. For extreme heat alone, using the baseline cutoff defined in section 2.3, we find that

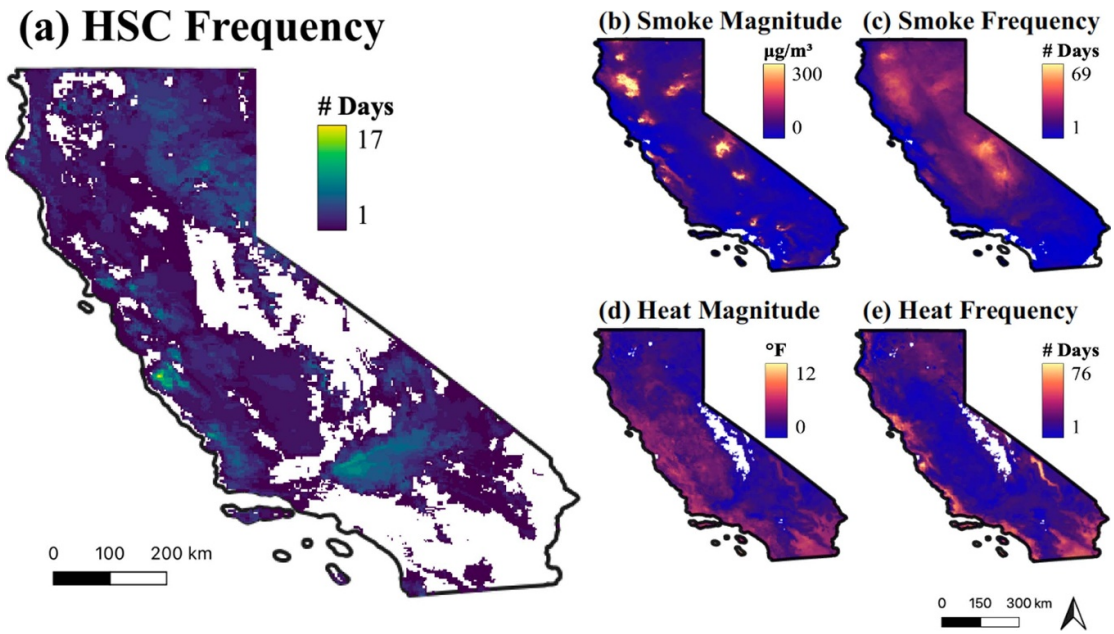

Figure 1. Spatial distribution of individual and co-occurring climate hazards. (a) The HSC map shows the frequency of HSC events in a given 3 km grid cell. Areas in white did not experience any event throughout the studied period. (b) The smoke magnitude displays the season's mean exceedance above 20 μg m^{-3} for each grid cell. (c) The smoke frequency displays the total number of days with smoke magnitudes exceeding the 'extreme' threshold of 20 μg m^{-3}. (d), (e) The same definitions for magnitude and frequency apply relative to each grid cell's 85th percentile historical heat index.

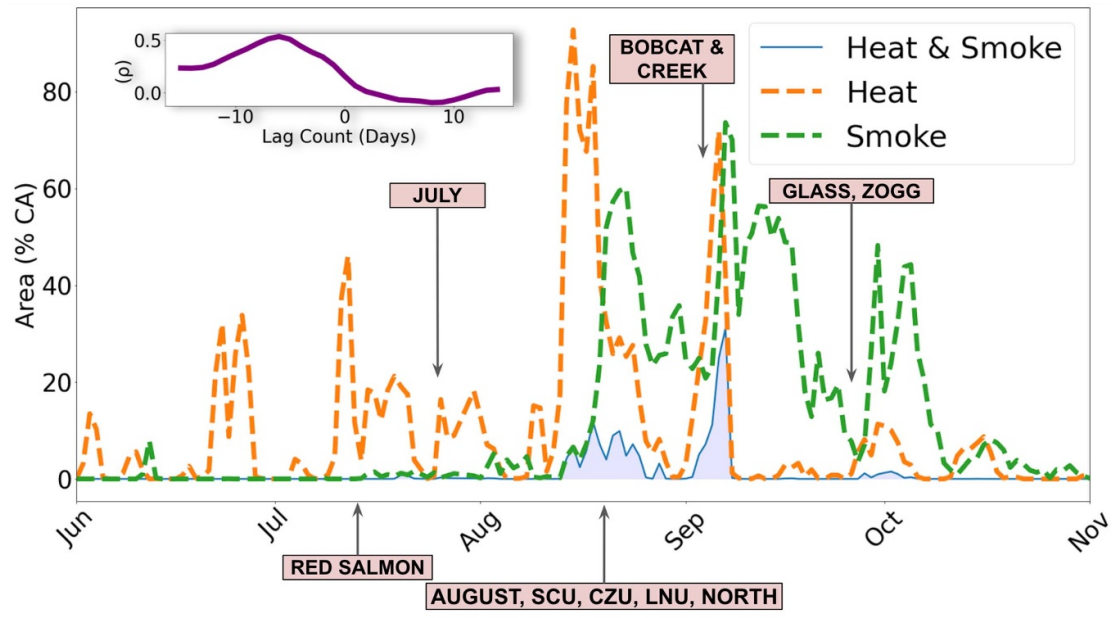

Figure 2. Area of California in extreme heat, smoke, and combined hazard categories for summer 2020. Dashed lines show the percent of California affected by individual hazard exceedances for the studied period. The solid blue line corresponds to the area of concurrent heat and smoke. Boxes with arrows indicate name and ignition dates of wildfires (±2 d). The inset line chart on the top left shows the cross-correlation between the daily area of heat and smoke exceedance at different time lags.

Mediterranean coastal regions as well as Desert areas in the Mojave were most frequently affected (table S1). These areas, in addition to the Central Valley, a primary agricultural region, also experienced the most intense heat events. For smoke $PM_{2.5}$, the season's average exceedance over the baseline threshold was greatest in Northwestern Forested Mountains, at 84.1 μg m^{-3}, and these events also lasted longest, for an average of 4.5 d. The exceedance magnitude in Forested areas was significantly larger than the next-most impacted Marine ecoregion ($\mu = 50.2$ μg m^{-3}).

Time-series analysis shows peak heat and smoke $PM_{2.5}$ during the months of August and September. The Pearson correlation coefficient between daily HSC and smoke areas ($\rho = 0.45$) was smaller than for HSC and

heat ($\rho = 0.63$). There is also a discernible lagged trend between hazards. Time-lagged cross correlation, which identifies the offset (number of days) at which cross-correlation is maximized between variables, peaks at 6 d for maximum heat index and smoke ($\rho = 0.57$). This suggests that an increase in the frequency of heat waves longer than six days may increase co-occurrences, assuming stationarity in heat-wildfire dynamics.

3.3. Sensitivity

There is a nonlinear decline in the frequency of HSC when we examine persistent smoke waves and/or heat waves. As table 1 illustrates, applying a persistence threshold of two or more consecutive exceedances for both smoke and heat diminishes the total HSC-affected area by 27% from ∼288 000 km^2 to approximately ∼211 000 km^2 of the State. This decline in area corresponds to a slightly larger 33% decline in the total affected population. Our results are also sensitive to the extreme heat and smoke thresholds—an increase from the 85th to 95th percentile decreases frequency-weighted affected area by nearly 60% and an increase in the smoke threshold from 20 μg m^{-3} to 35 μg m^{-3} results in a drop of 47%. For reference, the average 85th and 95th percentiles for maximum heat index in California correspond to 92 °F and 95 °F, respectively. Finally, persistent events, namely heat waves and smoke waves, are associated with more intense magnitudes, exceeding non-persistent scenarios by an average 9.5% and 10.4%, respectively.

3.4. Population exposure

Out of approximately 40 million residents, we estimate that 35.3, 30.2 and 16.5 million residents were affected by at least one occurrence of extreme heat, smoke and HSC, respectively (figure S3). Relative to the statewide average population density of 98.9 persons/km^2, heat-affected areas were denser ($\mu = 102.43$) and smoke-affected areas less dense ($\mu = 86.5$). Gridded areas with at least one HSC event had, on average, lower population densities ($\mu = 67.5$, $\sigma = 392.8$, $n = 40\,425$) than unaffected areas ($\mu = 171.3$, $\sigma = 771.7$, $n = 17\,735$).

Proportionality tests show that certain populations are overrepresented in areas with HSC compared to their total statewide representation (figure 3). Based on census demographic data from 2019, 'White Alone' respondents were 1.05 times as likely to be exposed to HSC than would be expected based on their overall share of the population. Conversely, 'Black or African American Alone' individuals, who represent 5.7% of the total population in California, represented 5.2% of the population exposed to HSC. Hispanic and Latino populations were even less likely to reside in HSC affected areas—comprising 39.2% of the State's population but only 34.0% of the affected population (table S3).

Last, we compare smoke and heat exceedance magnitudes with a series of sociodemographic and risk variables at the census tract level (table S2), namely the shares of the population that are White, Hispanic, African American and Native American; the percent of the population that suffers from cardiovascular illness; the level of poverty and linguistic isolation; summertime average 8 h maximums of ozone concentrations from 2017–2019; and the OEHAA's CalEnviroScreen score, a holistic score that combines an area's pollution burden with its population vulnerability. Among variables that show non-zero linear trends ($p < 0.01$), the largest observed magnitude was a decrease in the exceedance magnitude of temperature −0.1 °F for each decile increase in the summertime maximum ozone and −0.06 °F for each decile increase in the percent of the population that is White-identifying. Nearly all other variables' associations with smoke were less than ± 0.02 μg m^{-3} per decile increase or statistically insignificant.

4. Discussion

Our study shows that 68% of California's land area and 42% of the population simultaneously experienced hazardous smoke $PM_{2.5}$ and extreme temperatures at least once in 2020. While these results may represent an 'upper bound' considering 2020's wildfire season was the largest in California's modern history, four million burned acres was in fact typical for the state prior to European settlements and concomitant fire suppression (Safford *et al* 2022). These compound events peaked in August and lasted through October. The Forested ecoregion in northern California and neighboring Marine ecoregion, where large wildfires were observed in 2020, were most affected by HSC. These spatiotemporal patterns match findings from another smoke $PM_{2.5}$ exposure assessment in earlier years which, using a coarser smoke-specific model, found peak concentrations in August concentrated in northern California (Koman *et al* 2019). These patterns may be attributable to available fuel loads in these ecoregions, as well as differences in plant sensitivity to dryness that influence wildfire risk (McKinnon *et al* 2021, Rao *et al* 2022).

Overall, persistent HSC events (at least 2 d) were found to be more intense than single day hazard extremes. Hazard magnitudes were also found to be lower during HSC events than for individual hazards. This is likely attributable to the relatively temperate climates in which smoke events were concentrated. Notwithstanding, previous studies have found that milder climates with less adaptive capacity are similarly

Table 1. Sensitivity Analysis. (a) *Frequency weighted area* is the occurrence frequency of HSC in a given pixel, multiplied by the area of that pixel; (b) *minimum extent* is the percent of CA that experiences at least one HSC event in the studied timespan; (c) maximum pixel frequency is the maximum number of HSC events observed in a pixel, statewide; (d) *HSC average frequency* is the statewide average of all HSC counts among pixels with HSC counts greater than zero (i.e. unaffected areas are masked); (e) *mean heat magnitude* is the statewide mean of each pixel's seasonal mean exceedance above the heat threshold for days and locations with HSC; (f) *mean smoke magnitude* is the same as *e* but for smoke; (g) *HSC maximum persistence* is the largest observed consecutive run length of HSC events in a pixel throughout the state; (h) *HSC average persistence* is the same as *g* but the average; (i) *population affected* is the total number of people residing in locations that are within the minimum extent (see *b*).

Magnitude thresholds			Persistence threshold	HSC outcomes (statewide)								
Heat (%ile)	Smoke (μg m^{-3})	Heat metric	Heat & smoke (days)	Frequency weighted area (km^2-day)	Minimum extent (%)	HSC maximum frequency	HSC average frequency	Mean heat magnitude exceedance (°F)	Mean smoke magnitude exceedance (μg m^{-3})	HSC maximum persistence (days)	HSC average persistence (days)	Population affected (people)
85	20	max	0	7.2×10^{05}	68.1	17	2.5	2.6	40.9	9	1.6	1.7×10^{07}
85	20	min	0	1.7×10^{06}	79.7	26	5.1	4.0	47.5	22	1.9	1.8×10^{07}
95	20	max	0	2.8×10^{05}	35.8	13	1.8	2.2	29.9	8	1.4	8.4×10^{06}
95	20	min	0	8.2×10^{05}	63.4	21	3.0	3.2	50.3	11	1.6	1.2×10^{07}
85	35	max	0	3.8×10^{05}	48.6	12	1.9	2.3	54.9	8	1.4	8.9×10^{06}
85	35	min	0	1.1×10^{06}	65.7	22	3.9	3.9	58.6	19	1.8	1.1×10^{07}
95	35	max	0	1.3×10^{05}	20.0	8	1.5	1.8	44.5	6	1.3	3.4×10^{06}
95	35	min	0	4.8×10^{05}	48.2	14	2.4	3.1	64.0	10	1.4	7.0×10^{06}
85	20	max	2	5.2×10^{05}	49.6	12	2.5	2.8	46.8	9	2.0	1.1×10^{07}
85	20	min	2	1.4×10^{06}	68.9	26	4.9	4.1	53.2	22	2.3	1.4×10^{07}
95	20	max	2	1.9×10^{05}	21.8	9	2.0	2.4	32.5	8	1.7	5.7×10^{06}
95	20	min	2	6.1×10^{05}	47.4	20	3.0	3.5	47.5	11	1.9	7.7×10^{06}
85	35	max	2	2.5×10^{05}	31.0	8	1.9	2.6	63.4	8	1.8	5.4×10^{06}
85	35	min	2	8.5×10^{05}	53.8	22	3.7	3.9	68.0	19	2.2	8.6×10^{06}
95	35	max	2	7.2×10^{04}	10.1	6	1.7	2.3	54.2	6	1.6	1.4×10^{06}
95	35	min	2	3.3×10^{05}	31.6	13	2.5	3.4	64.8	10	1.8	3.6×10^{06}

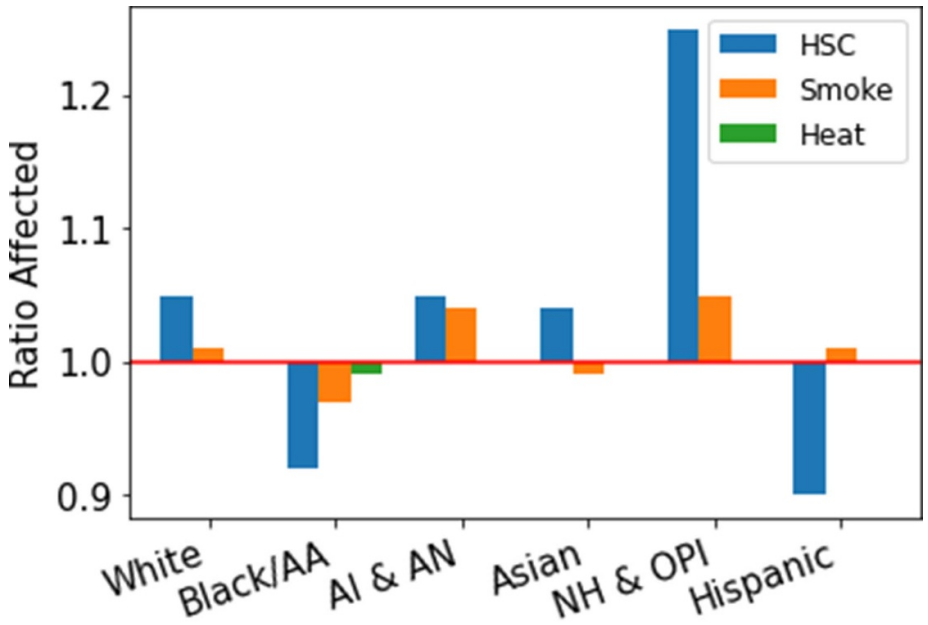

Figure 3. Proportionality. Bar plots show the ratio above or below one at which different ethnicities and races in California were affected by individual hazard exceedances and HSC, relative to their share of the general population. Abbreviations: Black & AA—Black and African American; AI & AN—American Indian and Alaska Native; NH & OPI—Native Hawaiian & Other Pacific Islander; Latino—Latino or Hispanic.

vulnerable to heightened morbidity and mortality from persistent heat exposure (Knowlton *et al* 2009). Finally, the average extreme smoke $PM_{2.5}$ concentration during HSC events was more than double the EPA's 24 h standard (35 μg m^{-3}) and presents a significant health risk to affected communities.

We do not find many associations between the amount of threshold exceedance for location-specific 'extremes' for heat and smoke and the selected sociodemographic covariates at the census-tract level. That is to say that no population group or social pattern was associated with a disproportionate increase or decrease in the intensity of extreme events. The lack of meaningful trends, especially in the smoke context, are likely because wildfire ignition and the subsequent meteorological conditions that influence smoke transport are stochastic and affect broad regions. Yet, in line with previous work that finds minority groups to be less exposed to wildfire (Burke *et al* 2021, Masri *et al* 2021), we similarly find evidence that white individuals are more likely to be exposed to concurrent heat and smoke. These predispositions are likely a result of certain groups' propensity to live in rural areas nearer smoke emitting fires.

There are several limitations to this analysis. Because there are no empirical datasets of surface-level smoke $PM_{2.5}$ across the State, we relied on short-term forecasts that inherently feature some imprecision. However, unlike observed measurements from AQS that cover a small fraction of the state in mostly urban areas, HRRR-Smoke is spatially continuous and isolates the fire contribution to pollution. Although our case study of California in 2020 is instructive due to the State's ecological diversity and size, our results cannot be directly translated to other geographies and years. Nonetheless, climate driven fire risk in California will only worsen through the middle of the century; seasons of similar intensity for both heat and smoke are therefore plausible, if not likely, to reoccur. Additionally, our heat index measurements, while based on observed temperatures, do not account for microclimate impacts or wind which are both known to shape heat stress during outdoor activities (Thorsson *et al* 2014). Finally, because we lack a definitive understanding of people's physiological and adaptive responses to varying intensities of heat and smoke, our analysis makes population-level assumptions about the magnitudes that may be considered hazardous.

5. Conclusion

We report population-level exposure for individual and co-occurring climate-related hazards and find that a majority of California's land area, especially ecoregions in northern California with dense fuel loads, were affected by HSC. The location of these events are unassociated with social indicators of vulnerability, however, they tend to cluster in rural areas near observed fire perimeters (figure S1). To our knowledge, this is the first study to describe the spatiotemporal dynamics of HSC throughout California and to examine their disproportionate impacts on certain communities in the State. We advance previous work by examining

exposures at a relatively high spatial resolution (3 km) with smoke-specific $PM_{2.5}$ estimates to isolate wildfire contributions from other sources of air pollution.

This study suggests several promising areas for future research. First, researchers can leverage this analysis to estimate the excess morbidity and mortality resulting from the *interactions* between heat and smoke $PM_{2.5}$ while accounting for mediating sociodemographic factors that may otherwise be obfuscated at coarser spatial resolutions. Second, longer-term studies can examine the meteorological and geophysical drivers of heat and smoke to identify multi-year HSC exposures as well as the causal mechanisms behind HSC, and in turn, enable better prediction. This would require an expanded time series of smoke $PM_{2.5}$ concentrations that is not currently available from the HRRR-Smoke model that became operational in 2020; therefore, other observational or modeling datasets are needed to backfill historical smoke patterns. Third, future climate change scenarios may alter HSC frequency and duration (Kalashnikov *et al* 2022), but future projection was beyond the scope of this analysis. Finally, we can further investigate the social drivers of differential exposure between racial and ethnic groups including housing stock, urban tree canopy cover and occupation.

With the intensity and duration of extreme heat events and wildfires projected to increase over the coming decades (Westerling 2016, 2018), HSC is likely to become increasingly frequent. Accordingly, public health officials must account for hazard interactions in their planning efforts and their potential to incur harms on human health that exceed the sum of their parts.

Data availability statement

The data that support the findings of this study are openly available at the following URL/DOI: https://code.earthengine.google.com/363e0bb05e60465962318951ab0f69b1.

Acknowledgments

We thank Professor Alan Barrecca and Professor Adam Millard-Ball for their support; Sierra Raby and Martha Salazar for their assistance with providing processed data for the smoke $PM_{2.5}$ analysis. This study was supported by the University of California Multicampus Research Programs and Initiatives (MRPI, MRP-17-446315); an award to M E M through the Google Research Scholar Program; and an award to N R from the Los Angeles Center for Urban Natural Resources Sustainability. M E M acknowledges financial interest in Google.

Code availability statement

The link to the Earth Engine module that hosts the data, performs all spatial analyses and exports image and tabular outputs in a self-contained environment can be found here: https://code.earthengine.google.com/363e0bb05e60465962318951ab0f69b1.

Contributions

N R and M E M designed the study. N R performed the analysis, designed and produced the figures and wrote the manuscript, with input from all co-authors.

ORCID iDs

Noam Rosenthal https://orcid.org/0000-0003-1303-4333
Tarik Benmarhnia https://orcid.org/0000-0002-4018-3089
Miriam E Marlier https://orcid.org/0000-0001-9333-8411

References

Abatzoglou J T 2013 Development of gridded surface meteorological data for ecological applications and modelling *Int. J. Climatol.* **33** 121–31

Abatzoglou J T and Williams A P 2016 Impact of anthropogenic climate change on wildfire across western US forests *Proc. Natl Acad. Sci.* **113** 11770–5

Aguilera R, Corringham T, Gershunov A and Benmarhnia T 2021 Wildfire smoke impacts respiratory health more than fine particles from other sources: observational evidence from Southern California *Nat. Commun.* **12** 1493

Ahmadov R *et al* 2017 Using VIIRS fire radiative power data to simulate biomass burning emissions, plume rise and smoke transport in a real-time air quality modeling system *2017 IEEE Int. Geoscience and Remote Sensing Symp. (IGARSS)* pp 2806–8

Austin E, Kasner E, Seto E and Spector J 2020 Combined burden of heat and particulate matter air quality in WA agriculture *J. Agromedicine* **26** 1–10

Brook R D *et al* 2010 Particulate matter air pollution and cardiovascular disease *Circulation* **121** 2331–78
Burke M, Driscoll A, Heft-Neal S, Xue J, Burney J and Wara M 2021 The changing risk and burden of wildfire in the United States *Proc. Natl Acad. Sci. USA* **118** e2011048118
CalFire 2020 2020 Fire Siege (available at: www.fire.ca.gov/media/hsviuuv3/cal-fire-2020-fire-siege.pdf)
Cheng J, Xu Z, Bambrick H, Prescott V, Wang N, Zhang Y, Su H, Tong S and Hu W 2019 Cardiorespiratory effects of heatwaves: A systematic review and meta-analysis of global epidemiological evidence *Environ. Res.* **177** 108610
Chow F K *et al* 2021 High-resolution smoke forecasting for the 2018 camp fire in California *Bull. Am. Meteorol. Soc.* **1** E1531–52
Center for International Earth Science Information Network - CIESIN - Columbia University 2018 *Population Estimation Service, Version 3 (PES-v3)* (Palisades, NY: NASA Socioeconomic Data and Applications Center (SEDAC)) (https://doi.org/10.7927/H4DR2SK5)
Davies P and Maconochie I 2009 The relationship between body temperature, heart rate and respiratory rate in children *Emerg. Med. J.* **26** 641–3
DeFlorio-Barker S, Crooks J, Reyes J and Rappold A G 2019 Cardiopulmonary effects of fine particulate matter exposure among older adults, during wildfire and non-wildfire periods, in the United States 2008–2010 *Environ. Health Perspect.* **127** 037006
Ebi K L *et al* 2021 Hot weather and heat extremes: health risks *Lancet* **398** 698–708
Field C B, Barros V, Stocker T F and Dahe Q (eds) 2012 *Managing the Risks of Extreme Events and Disasters to Advance Climate Change Adaptation: Special Report of the Intergovernmental Panel on Climate Change* (Cambridge: Cambridge University Press) (https://doi.org/10.1017/CBO9781139177245)
Ford B, Val Martin M, Zelasky S E, Fischer E V, Anenberg S C, Heald C L and Pierce J R 2018 Future fire impacts on smoke concentrations, visibility, and health in the contiguous United States *GeoHealth* **2** 229–47
Gill J C and Malamud B D 2014 Reviewing and visualizing the interactions of natural hazards *Rev. Geophys.* **52** 680–722
Gorelick N, Hancher M, Dixon M, Ilyushchenko S, Thau D and Moore R 2017 Google earth engine: planetary-scale geospatial analysis for everyone *Remote Sens. Environ.* **202** 18–27
Goss M, Swain D L, Abatzoglou J T, Sarhadi A, Kolden C A, Williams A P and Diffenbaugh N S 2020 Climate change is increasing the likelihood of extreme autumn wildfire conditions across California *Environ. Res. Lett.* **15** 094016
Guo C *et al* 2018 Effect of long-term exposure to fine particulate matter on lung function decline and risk of chronic obstructive pulmonary disease in Taiwan: a longitudinal, cohort study *Lancet Plan. Health* **2** e114–e125
Heaney A, Stowell J D, Liu J C, Basu R, Marlier M and Kinney P 2022 Impacts of fine particulate matter from wildfire smoke on respiratory and cardiovascular health in California *GeoHealth* **6**
Hoshiko S, English P, Smith D and Trent R 2010 A simple method for estimating excess mortality due to heat waves, as applied to the 2006 California heat wave *Int. J. Public Health* **55** 133–37
Jacklitsch B, Musolin K, Williams J, Coca A, Kim J-H and Turner N 2016 Criteria for a recommended standard: occupational exposure to heat and hot environments (https://doi.org/10.1080/15459624.2016.1179388)
Kalashnikov D A, Schnell J L, Abatzoglou J T, Swain D L and Singh D 2022 Increasing co-occurrence of fine particulate matter and ground-level ozone extremes in the western United States *Sci. Adv.* **8**
Keatinge W R, Coleshaw S R, Easton J C, Cotter F, Mattock M B and Chelliah R 1986 Increased platelet and red cell counts, blood viscosity, and plasma cholesterol levels during heat stress, and mortality from coronary and cerebral thrombosis *Am. J. Med.* **81** 795–800
Knowlton K, Rotkin-Ellman M, King G, Margolis H G, Smith D, Solomon G, Trent R and English P 2009 The 2006 California heat wave: impacts on hospitalizations and emergency department visits *Environ. Health Perspect.* **117** 61–67
Koman P D, Billmire M, Baker K R, de Majo R, Anderson F J, Hoshiko S, Thelen B J and French N H F 2019 Mapping modeled exposure of wildland fire smoke for human health studies in California *Atmosphere* **10** 308
Liu J C *et al* 2017 Wildfire-specific fine particulate matter and risk of hospital admissions in urban and rural Counties *Epidemiology* **28** 77–85
Masri S, Scaduto E, Jin Y and Wu J 2021 Disproportionate impacts of wildfires among elderly and low-income communities in California from 2000–2020 *Int. J. Environ. Res. Public Health* **18** 3921
Mazdiyasni O and AghaKouchak A 2015 Substantial increase in concurrent droughts and heatwaves in the United States *Proc. Natl Acad. Sci. USA* **112** 11484–9
McKinnon K A, Poppick A and Simpson I R 2021 Hot extremes have become drier in the United States Southwest *Nat. Clim. Change* **11** 598–604
Moftakhari H R, Salvadori G, AghaKouchak A, Sanders B F and Matthew R A 2017 Compounding effects of sea level rise and fluvial flooding *Proc. Natl Acad. Sci. USA* **114** 9785–90
Nakayama Wong L S, Aung H H, Lamé M W, Wegesser T C and Wilson D W 2011 Fine particulate matter from urban ambient and wildfire sources from California's San Joaquin Valley initiate differential inflammatory, oxidative stress, and xenobiotic responses in human bronchial epithelial cells *Toxicol. Vitro* **25** 1895–905
National Centers for Environmental Information (NCEI) 2020 National Temperature and Precipitation Maps (available at: www.ncei.noaa.gov/access/monitoring/us-maps/3/202008?products[]=statewidetavgrank) (Accessed 1 September 2021)
National Weather Service 2014 Heat index equation (available at: www.wpc.ncep.noaa.gov/html/heatindex_equation.shtml) (Accessed 21 February)
Nielsen E R, Herman G R, Tournay R C, Peters J M and Schumacher R S 2015 Double impact: when both tornadoes and flash floods threaten the same place at the same time *Weather Forecast.* **30** 1673–93
O'Dell K, Ford B, Fischer E V and Pierce J R 2019 Contribution of wildland-fire smoke to US PM2.5 and its influence on recent trends *Environ. Sci. Technol.* **53** 1797–804
OEHHA 2021 California Communities Environmental Health Screening Tool *CalEnviroScreen 4.0* (available at: https://oehha.ca.gov/media/downloads/calenviroscreen/report/calenviroscreen40reportf2021.pdf) (Accessed November 2021)
Omernik J M 1987 Ecoregions of the conterminous United States *Ann. Assoc. Am. Geogr.* **77** 118–25
Perkins S E, Alexander L V and Nairn J R 2012 Increasing frequency, intensity and duration of observed global heatwaves and warm spells *Geophys. Res. Lett.* **39**
Rao K, Williams A P, Diffenbaugh N S, Yebra M and Konings A G 2022 Plant-water sensitivity regulates wildfire vulnerability *Nat. Ecol. Evol.* **6** 332–9
Rey G, Jougla E, Fouillet A, Pavillon G, Bessemoulin P, Frayssinet P, Clavel J and Hémon D 2007 The impact of major heat waves on all-cause and cause-specific mortality in France from 1971 to 2003 *Int. Arch. Occup. Environ. Health* **80** 615–26

Rothfusz L P 1990 The heat index 'equation' (or, more than you ever wanted to know about heat index) *NWS Technical Attachment SR 90–23* p 2

Safford H D, Paulson A K, Steel Z L, Young D J N and Wayman R B 2022 The 2020 California fire season: a year like no other, a return to the past or a harbinger of the future? *Glob. Ecol. Biogeogr.* 1–21

Schwarz L, Hansen K, Alari A, Ilango S D, Bernal N, Basu R, Gershunov A and Benmarhnia T 2021 Spatial variation in the joint effect of extreme heat events and ozone on respiratory hospitalizations in California *Proc. Natl Acad. Sci.* **118**

Schwarz L, Malig B, Guzman-Morales J, Guirguis K, Ilango S D, Sheridan P, Gershunov A Basu R and Benmarhnia T 2020 The health burden fall, winter and spring extreme heat events in the in Southern California and contribution of Santa Ana Winds *Environ. Res. Lett.* **15** 054017

Sherbakov T, Malig B, Guirguis K, Gershunov A and Basu R 2018 Ambient temperature and added heat wave effects on hospitalizations in California from 1999 to 2009 *Environ. Res.* **160** 83–90

Thorsson S, Rocklöv J, Konarska J, Lindberg F, Holmer B, Dousset B and Rayner D 2014 Mean radiant temperature—a predictor of heat related mortality *Urban Climate, ICUC8: The 8th Int. Conf. on Urban Climate and the 10th Symp. on the Urban Environment* vol 10 pp 332–45

U.S. Census Bureau 2019 *2014–2018 American Community Survey 5-Year. Retrieved from Social Explorer* (Accessed November 2020)

US EPA O 2014 NAAQS table (available at: www.epa.gov/criteria-air-pollutants/naaqs-table) (Accessed 29 December 2021)

US EPA O 2021 Climate change indicators: heat waves (available at: www.epa.gov/climate-indicators/climate-change-indicators-heat-waves) (Accessed 29 December 2021)

Westerling A L 2016 Increasing western US forest wildfire activity: sensitivity to changes in the timing of spring *Phil. Trans. R. Soc.* B **371** 20150178

Westerling A L 2018 *Wildfire Simulations for California's Fourth Climate Change Assessment: Projecting Changes in Extreme Wildfire Events with a Warming Climate. California's Fourth Climate Change Assessment* Rep. CCCA4-CEC-2018-014 (California Energy Commission) p 57 (available at: www.energy.ca.gov/sites/default/files/2019-11/Projections_CCCA4-CEC-2018-014_ADA.pdf)

Weuve J, Bennett E E, Ranker L, Gianattasio K Z, Pedde M, Adar S D, Yanosky J D and Power M C 2021 Exposure to air pollution in relation to risk of dementia and related outcomes: an updated systematic review of the epidemiological literature *Environ. Health Perspect.* **129** 096001

Ye X *et al* 2021 Evaluation and intercomparison of wildfire smoke forecasts from multiple modeling systems for the 2019 williams flats fire *Atmos. Chem. Phys.* **21** 14427–69

Zhang K, Rood R B, Michailidis G, Oswald E M, Schwartz J D, Zanobetti A, Ebi K L and O'Neill M S 2012 Comparing exposure metrics for classifying 'dangerous heat' in heat wave and health warning systems *Environ. Int.* **46** 23–29

Zscheischler J *et al* 2020 A typology of compound weather and climate events *Nat. Rev. Earth Environ.* **1** 333–47